Journal of Alloys and Compounds 509 (2011) 9123–9126

Contents lists available at ScienceDirect

Journal of Alloys and Compounds

journal homepage: www.elsevier.com/locate/jallcom

Magnetic and electric properties of C–Co thin films prepared by vaccum arc technique

A. Tembre[a], M. Clin[a], J.-C. Picot[a], J.-L. Dellis[a,*], J. Henocque[a], R. Bouzerar[b], K. Djellab[c]

[a] Laboratoire de Physique de la Matière Condensée, Université de Picardie Jules Verne, 33 rue Saint Leu, 80039 Amiens, France
[b] Laboratoire de Physique des Systèmes Complexes, Université de Picardie Jules Verne, 33 rue Saint leu, 80039 Amiens, France
[c] Plate-forme de Microscopie Electronique, Université de Picardie Jules Verne, 33 rue Saint Leu, 80039 Amiens, France

ARTICLE INFO

Article history:
Received 15 April 2010
Received in revised form 14 June 2011
Accepted 16 June 2011
Available online 6 July 2011

Keywords:
Amorphous materials
Thin films
Pulsed electric arc technique
Magnetic properties

ABSTRACT

Cobalt doped carbon thin films have been deposited by a pulsed anodic electric arc technique. The films were characterized by high resolution transmission electron microscopy, electric measurements under dc magnetic fields, and ac magnetic susceptibility measurements within a temperature range 15–300 K. An insulating to a metallic state transition at a critical temperature around 60 K was observed.

1. Introduction

In the past two decades, nanocrystalline magnetic materials made of metallic nanoclusters dispersed in an amorphous matrix have attracted considerable interest owing to their electrical [1–3] and magnetical [4–7] properties for applications such as sensors, electrode devices, optic components and for fundamental research [8,9].

Hayashi et al. [10] have reported the fabrication and characterization of magnetic thin films of h.c.p. cobalt nanocrystals of around 8 nm size encapsulated in graphite-like carbon cages. The cobalt grains had ferromagnetic nature thus has great potential for ultra-high-density magnetic recording media.

It has been reported that insertion of metallic atoms in an amorphous carbon matrix increases the fraction of Csp^3 coordinated carbon to the detriment of Csp^2 sites [11]. The incorporation in the carbon network of various metallic atoms, like Ti, Zr, Ta, Cr, Mo, W, Fe, Co, Ni, is a good alternative to improve the tribological [12–16], electric [17–21] and magnetic [22–28] properties of carbon films for various applications as solid lubricant films, microelectrodes or magnetic films.

Various techniques have been used to fabricate metallic nanoclusters dispersed in an amorphous matrix, such as filtered cathodic vacuum arc deposition [29–31], pulsed laser deposition [32], co-sputtering [21,33], dual beam evaporation [14], chemical vapor deposition [34,35] and detonation [36,37]. Among these different methods, cathodic arc deposition [38,39] is characterized by a high degree of ionization, large ion kinetic energy and a high deposition rate. Cathodic arc processes produce unwanted macroparticles in the μm range which can be removed from the plasma by a magnetic filter. On the contrary, anodic arcs do not suffer from macroparticle contamination, which was the main motivation of using this deposition technique in the present study. However, this anodic technique leads to low cobalt deposition rates.

In this paper, we report investigations on the electric and magnetic properties of cobalt doped carbon thin films deposited by DC pulsed anodic arc deposition for pure carbon and 0.3% cobalt samples whose properties were representative of all the samples we prepared.

2. Experimental details

2.1. Sample preparation

The cobalt doped carbon films were deposited by a home made pulsed anodic electric arc system, using graphite rod electrodes of 6 mm diameter. The anode was made of pure graphite rod packed with Co/C powder in a hole of 2 mm diameter in the center of the rod. The cathode was made of pure graphite rod. Both purities of graphite and cobalt powder were 99.9%. The anodic arc is triggered when cathode and anode touch each other. The arc current was 70 A and dc discharge voltage was 40 V with an arc duration of 1 s and pulse repetition rate of 5 Hz. A bias voltage of dc −400 V was applied to the subtrate holder. The base pressure of the deposition chamber was 0.1 Pa. The content of cobalt in carbon films were determined by atomic absorption using a PerkinElmer A. Analyst 300 apparatus. The weight ratio of cobalt

* Corresponding author.
E-mail address: jean-luc.dellis@u-picardie.fr (J.-L. Dellis).

0925-8388/$ – see front matter © 2011 Elsevier B.V. All rights reserved.
doi:10.1016/j.jallcom.2011.06.068

to carbon is found to be 0.3%. This cobalt content is monitored by the percentage cobalt (here 26%) in the Co/C powder used to made the anode.

The substrates were crystalline silicon [1 0 0] and glass, cleaned by degreasing in successive ultrasonic baths of trichloroethylene, acetone and methanol. The thicknesses of the deposited films, determined using a Dektak 3 profilometer, were about 200 nm.

2.2. Microscope observations and analyses

The films surface has been observed using a scanning electron microscope with a field emission gun (FEG, SEM, Quanta 200F) equipped with a microanalysis probe. The nanostructures of the films were observed by high resolution transmission electron microscopy (HRTEM) equipped with a microanalysis probe, at an accelerating voltage of 200 kV.

2.3. Electrical measurements

The electrical conductivity measurements were conducted in the coplanar configuration using an impedance spectrometer (Solartron SI 1260) in the frequency range from 1 Hz to 1 MHz, and temperature range of 15–300 K supplied by a Displex DE 202 cryogenerator. The Nyquist diagram at each temperature was interpreted within a parallel RC model, from which the electrical conductivity as a function of temperature was deduced. These studies were supplemented by conductance relaxation measurements, that is time variations of the conductance for fixed temperature, frequency and magnetic field.

2.4. Magnetic measurements

The magnetic susceptibility measurements were carried out in the same thermal and excitation frequency conditions. The susceptometer consists of a primary coil (made of about 20 turns) excited by the variable current supplied by a current source driven by an ac voltage generator. The small alternating magnetic field along the axis of the primary coil excites the sample occupying one of the two compartments of a secondary compensated coil. The voltage induced across the secondary coil is dominated by the sample's magnetic response.

3. Results and discussion

3.1. HRTEM studies

We present in Fig. 1, HRTEM image of the 0.3% cobalt sample, showing a region with curved fringes representing fullerene like graphitic (graphene) layers with the spacing of 0.34 nm. Structures with interlayer separation of 0.37 nm, could be attributed to chaoite, and regions containing a mixture of amorphous and crystallized phases show a complex microstructure due to the deposition method used. The presence of cobalt was confirmed by microanalysis probe data, and a few misoriented regions well crystallized of an average size of approximately 5 nm corresponding to a fringe spacing of 0.22 nm close to that of the interlayer separation in hcp Co (1 0 0) were observed.

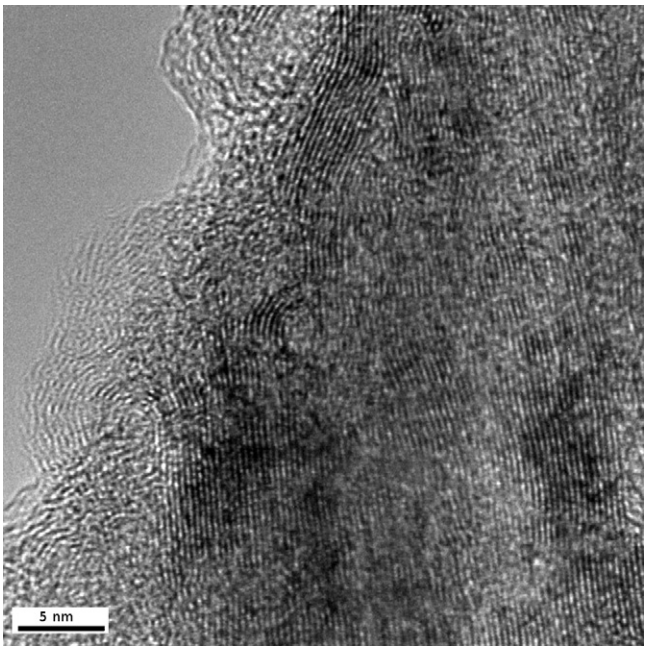

Fig. 1. HRTEM image obtained for 0.3% cobalt doped carbon thin film. Regions with curved fringes of fullerene like graphitic layers can be seen.

3.2. Metal–insulator transition

We present in Fig. 2 the variation of the electrical conductivity as a function of temperature deduced from the Nyquist diagrams obtained at each temperature. For the 0.3% cobalt sample, in the range of temperature 60–300 K, the conductivity curve increases with the increase of temperature. However, below 60 K the oppo-

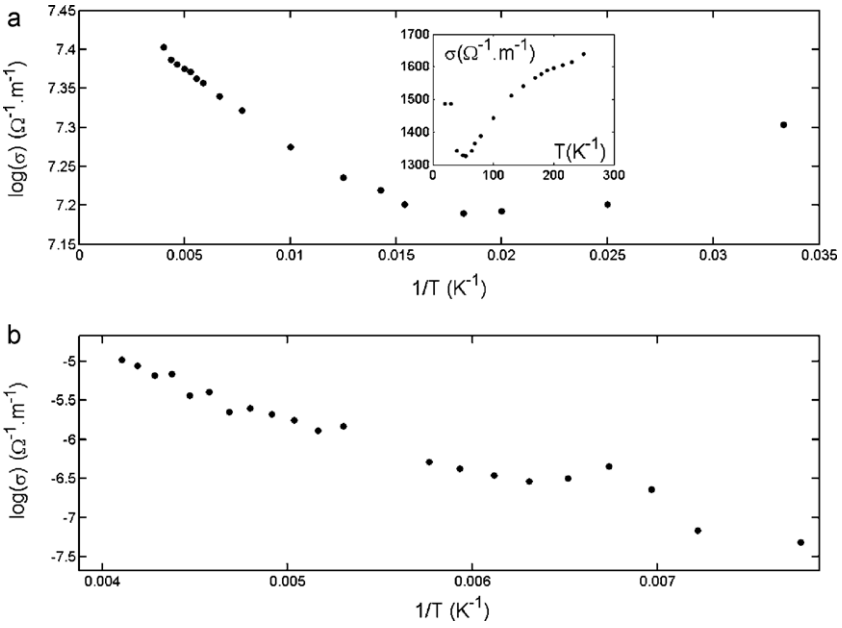

Fig. 2. The Arrhenius plots of the conductivity as a function of the inverse of temperature for (a) carbon/cobalt (0.3%); the insert shows the crossover temperature at around 60 K and (b) pure carbon.

site takes place. The crossover temperature at around 60 K indicates the possibility of a metal–insulator transition. The origin of this transition is probably due to the increase of the number of nanocrystalline graphitic clusters induced by the presence of cobalt in the semiconductor amorphous matrix. This assumption is supported by the recent Raman study we undertook and whose the results will be published in a separate article. The activation energy E_a and pre-factor σ_0 in the Arrhenius plot have been calculated, the values obtained (E_a = 1.7 meV and σ_0 = 1700 S m^{-1}) are in agreement with those reported by Takeno et al. [21]. In order to confirm the electrical anomaly around 60 K, direct impedance measurements were carried out in the temperature range 15–300 K on the 0.3% cobalt sample.

The impedance measurements consisted in recording the dynamical response of the film to a small amplitude alternating voltage of about 5 mV. This generates a response-current providing information on the films' physical properties. Processing these current data with a lock-in amplifier allows us to obtain the samples admittance formed by the in-phase and quadrature response (or equivalently to a conductance and a capacitance). It should be noted that the condition of a 'small' amplitude excitation voltage is essential since, this voltage being a probe, the perturbation of the electronic states involved in the response must be minimized. We used a field-cooled procedure in which we maintain the excitation across the junction on cooling the sample. The data were then recorded during the cooling and the heating steps. The heating and the cooling rate were fixed at a value of about 3 K/min, low enough to avoid any kinetic thermal inertia effects on the measurements.

The typical thermal evolution of the resistance $1/G(T, \omega)$ extracted from the real part of the admittance of the films at different dc magnetic fields is presented in Fig. 3. These curves exhibit a well defined low temperature plateau over the temperature range 15–45 K followed by a remarkable "anomaly" at about 60 K. This anomaly manifests itself as a resistance maximum on the "heated" curves. The resistance amplitude seems to be sensitive to external magnetic fields though the anomalous temperature shift remains weak. The resistance curves show the sample to be metal-like below the anomalous temperature while it is insulating above. This suggests an interpretation of this temperature as a critical threshold for a metal–insulator transition. Support for this hypothesis are provided by conductance relaxation measurements. Typical examples of these curves (obtained at 17 Hz) are presented in Fig. 4.

These were obtained for zero magnetic field at a frequency fixed at 17 Hz between 25 and 150 K. At low temperatures, the conductance does not vary with time. Just below the anomalous temperature (curves at 40 K), the conductance decreases (the resistance increases). At 50 K and above, we observe a reversed relaxation with time: the conductance increases with a long relaxation time. The limit between these two relaxational regimes takes place at 45 K, the temperature at which the onset occurs of the low temperature plateau of the resistance (see Fig. 3) or of the capacitance. We are thus led to distinguish this thermal onset as a new critical threshold for a metal–insulator transition and merits further study.

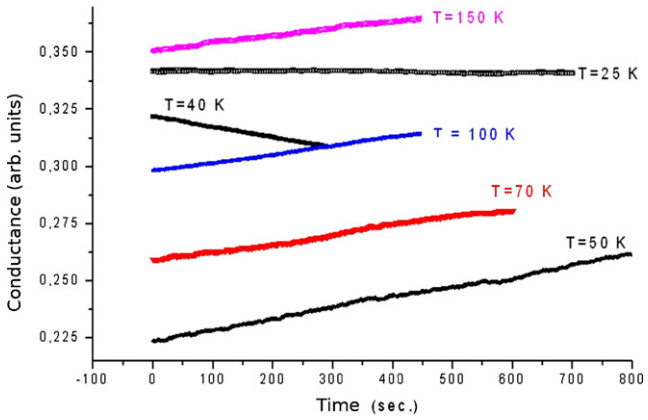

Fig. 4. Changes of the conductance relaxational dynamics within the temperature range 25–150 K.

3.3. Magnetic susceptibility measurements

The main conclusions drawn from the resistance measurements in magnetic field carried out on the 0.3% Co sample concerns the anomalous behaviour observed within the temperature range 45–150 K. Our assumption of a metal–insulator transition taking place are confirmed by ac magnetic susceptibility measurements.

The thermal evolution of the real part of the susceptibility $\chi'(\omega,T)$ (at a frequency ω) for the 0.3% Co sample is reported in Fig. 5. Upon heating, the susceptibility exhibits a peak around 60 K coinciding with the resistance maximum. Above 150 K, the curves obtained upon heating and cooling coincide, similarly to the resistance. At high temperatures, the susceptibility seems to be constant and negative. Nevertheless, we hesitate to attribute this negative constant value to diamagnetism. The diamagnetic contribution, which is always present, can arise from the capsule containing the powdered sample. But even when this unwanted component is substracted, the remaining magnetic response of the sample mixes a

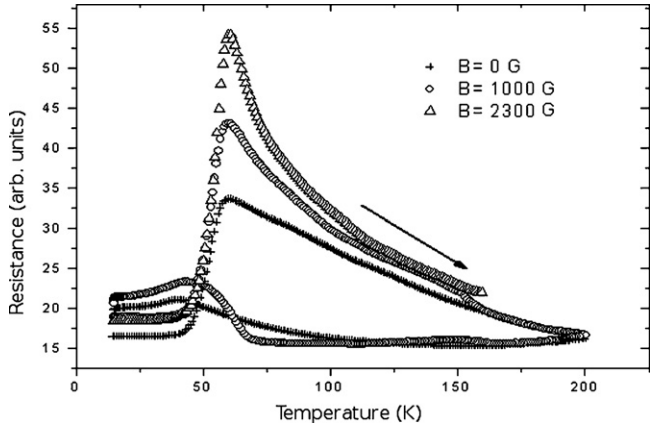

Fig. 3. Thermal hysteresis of the resistance for the 0.3% cobalt sample under various magnetic fields. The presence of a maximum resistance suggests a metal–insulator transition.

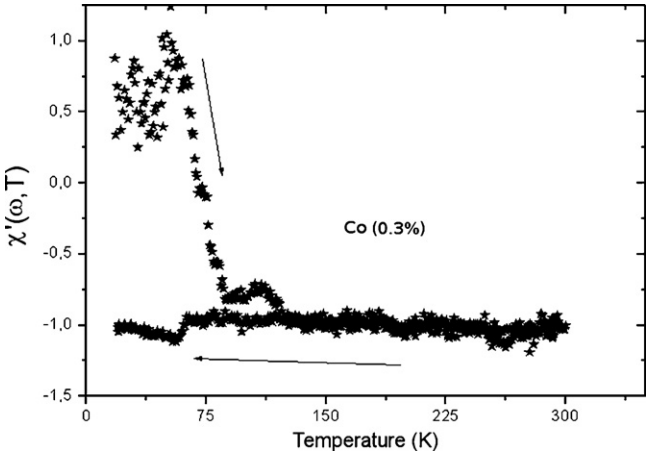

Fig. 5. Thermal hysteresis of the real part of the magnetic susceptibility for the 0.3% cobalt doped carbon film.

diamagnetic component and a paramagnetic one. A deeper analysis of these results is thus necessary and requires specific precautions to conclude on the nature of the observed magnetic state.

These results are compared with those of Kumari et al. [40,41] on iodine doped amorphous carbon prepared by vapor phase pyrolysis. Iodine incorporation and pyrolysis temperature induced a transition from an insulating to metallic state at about 21 K. Although fullerene and chaoite phases have shown ferromagnetic behaviour [42], the pure carbon films containing these phases did not exhibit a magnetic anomaly in our study. Consequently, the observed magnetic behaviour is due to the presence of cobalt in our films.

4. Summary

Cobalt doped carbon thin films were produced by a vacuum anodic arc discharge technique. Observation by HRTEM revealed that the films were composed of well crystallized cobalt layers and complex graphitic microstructure. Electrical measurements show a maximum resistance around 60 K, suggesting a metal–insulator transition on the 0.3% cobalt sample. Magnetic susceptibility measurements show anomalous behaviour around 60 K.

Acknowledgements

The authors would like to thank Dr. D. Larcher, and C. Surcin for technical assistance.

References

[1] I.H. Gul, A. Maqsood, M. Naeem Ashiq, J. Alloys Compd. 507 (2010) 201.
[2] S. Mahendia, A.K. Tomar, S. Kumar, J. Alloys Compd. 508 (2010) 406.
[3] S.U. Jen, H.P. Chiang, H.D. Liu, C.C. Chang, J. Alloys Compd. 508 (2010) 528.
[4] Y. Wang, F. Xiu, Y. Wang, X. Kou, P. Ajey, A.P. Jacob, L. Kang, K.L. Wang, J. Zou, J. Alloys Compd. 508 (2010) 273.
[5] V. Goyal, K.P. Bhatti, S. Chaudhary, J. Alloys Compd. 508 (2010) 419.
[6] J.-J. Gu, J.-J. Liu, H.-T. Li, Q. Xu, H.-Y. Sun, J. Alloys Compd. 508 (2010) 516.
[7] A. Ali Ghasemi, E. Ghasemi, J. Alloys Compd. 508 (2010) 565.
[8] P. Stamp, Nature 359 (1992) 365.
[9] B. Barbara, J. Magn. Magn. Mater. 156 (1996) 123.
[10] T. Hayashi, S. Hirono, M. Tomita, S. Umemura, Nature 381 (1996) 792.
[11] J. Robertson, Mater. Sci. Eng. R 37 (2002) 129–281.
[12] Q. Wei, R.J. Narayan, J. Narayan, T. Sankar, A.K. Sharma, Mater. Sci. Eng. B 53 (1998) 262.
[13] X. Han, F. Yan, A. Zhang, P. Yan, B. Wang, W. Liu, Z. Mu, Mater. Sci. Eng. A 348 (2003) 319.
[14] X. Nie, J.C. Jiang, L.D. Tung, L. Spinu, E.I. Meletis, Thin Solid Films 415 (2002) 211.
[15] V.V. Uglova, V.M. Anishchik, Y. Pauleau, A.K. Kuleshov, F. Thiery, J. Pelletier, S.N. Dub, D.P. Rusalsky, Vacuum 70 (2003) 181.
[16] G.J. Kovacs, G. Safran, O. Geszti, T. Ujvari, I. Bertoti, G. Radnoczi, Surf. Coat. Technol. 180–181 (2004) 331.
[17] E. Liu, X. Shi, L.K. Cheah, Y.H. Hu, H.S. Tan, J.R. Shi, B.K. Tay, Solid State Electron. 43 (1999) 425.
[18] J.C. Orlianges, C. Champeaux, A. Catherinot, A. Pothier, F. Blondy, P. Abelard, B. Angleraud, Thin Solid Films 453–454 (2004) 291.
[19] T. Takeno, H. Miki, T. Takagi, H. Onodera, Diamond Relat. Mater. 15 (2006) 1902.
[20] G. Schultes, P. Frey, D. Goettel, O. Freitag-Weber, Diamond Relat. Mater. 15 (2006) 80.
[21] T. Takeno, Y. Hoshi, H. Miki, T. Takagi, Diamond Relat. Mater. 17 (2008) 1669.
[22] J.M. Bonard, S. Seraphin, J.E. Wegrowe, J. Jiao, A. Chatelain, Chem. Phys. Lett. 343 (2001) 251.
[23] W.B. Mi, L. Guo, E.Y. Jiang, Z.Q. Li, P. Wu, H.L. Bai, J. Phys. D: Appl. Phys. 36 (2003) 2393.
[24] Z. Zhukova, J.M. Blanco, A. Zhukov, J. Conzalez, A. Torcunov, V. Larin, J. Magn. Magn. Mater. 254–255 (2003) 94.
[25] Z.H. Wang, Z.D. Zhang, C.J. Choi, B.K. Kim, J. Alloys Compd. 361 (2003) 289.
[26] J. Ling, Y. Liu, G. Hao, X. Zhang, Mater. Sci. Eng. B 100 (2003) 186.
[27] H. Wang, M.F. Chiah, W.Y. Cheung, S.P. Wong, Phys. Lett. A 316 (2003) 122.
[28] N. Nishi, K. Kosugi, K. Hino, T. Yokoyama, E. Okunishi, Chem. Phys. Lett. 369 (2003) 198.
[29] D.H.C. Chua, W.I. Milne, B.K. Tay, P. Zhang, X.Z. Ding, J. Vac. Sci. Technol. A 21 (2003) 353.
[30] R.K.Y. Fu, Y.F. Mei, L.R. Shen, G.G. Siu, P.K. Chu, W.Y. Cheung, S.P. Wong, Surf. Coat. Technol. 186 (2004) 112.
[31] M.-H. Teng, S.-W. Tsai, C.-I. Hsiao, Y.-D. Chen, J. Alloys Compd. 434–435 (2007) 678.
[32] N. Benchikh, F. Garrelie, K. Wolski, C. Donnet, R.Y. Fillit, F. Rogemond, J.L. Subtil, J.N. Rouzaud, J.Y. Laval, Thin Solid Films 494 (2006) 98.
[33] P. Dubcek, N. Radic, O. Milat, Nucl. Instrum. Methods Phys. Res. B 200 (2003) 329.
[34] H. Li, N. Zhao, C. He, C. Shi, X. Du, J. Li, J. Alloys Compd. 458 (2008) 130.
[35] J.L. Qi, X. Wang, H.W. Tian, Y.S. Peng, C. Liu, W.T. Zheng, J. Alloys Compd. 486 (2009) 265.
[36] G. Sun, X. Li, Y. Zhang, X. Wang, D. Jiang, F. Mo, J. Alloys Compd. 473 (2009) 212.
[37] N. Luo, X. Li, X. Wang, H. Yan, C. Zhang, H. Wang, Carbon 48 (2010) 3858.
[38] A. Anders, J. Phys. D: Appl. Phys. 40 (2007) 2272.
[39] P.J. Martin, A. Bendavid, Thin Solid Films 394 (2001) 1.
[40] L. Kumari, S.V. Subramanyam, J. Appl. Phys. 99 (2006) 096107.
[41] L. Kumari, S.V. Subramanyam, S. Eto, K. Takai, T. Enoki, Carbon 42 (2004).
[42] S. Li, Z. Huang, L. Lü, F. Zhang, Y. Du, Y. Cai, Y. Pan, Appl. Phys. Lett. 90 (2007) 232507.